XVI CONGRESSO SOCIETÀ OFTALMOLOGICA CALABRESE SOC

CORSO AVANZATO DI SEMEIOTICA STRUMENTALE
XVI Congresso Società Oftalmologica Calabrese

Strumentazioni Hi-Tech e piattaforme d'integrazione

Simone Donati

Department of Ophthalmology
University of Insubria, Varese - Italy
Chairman: Claudio Azzolini MD

Agenda

- Strumentazioni Hi-Tech: che cosa?
- Quali patologie?
- Come lavorano?
- Nuovi strumenti: nuovi problemi

Wide Field Imaging

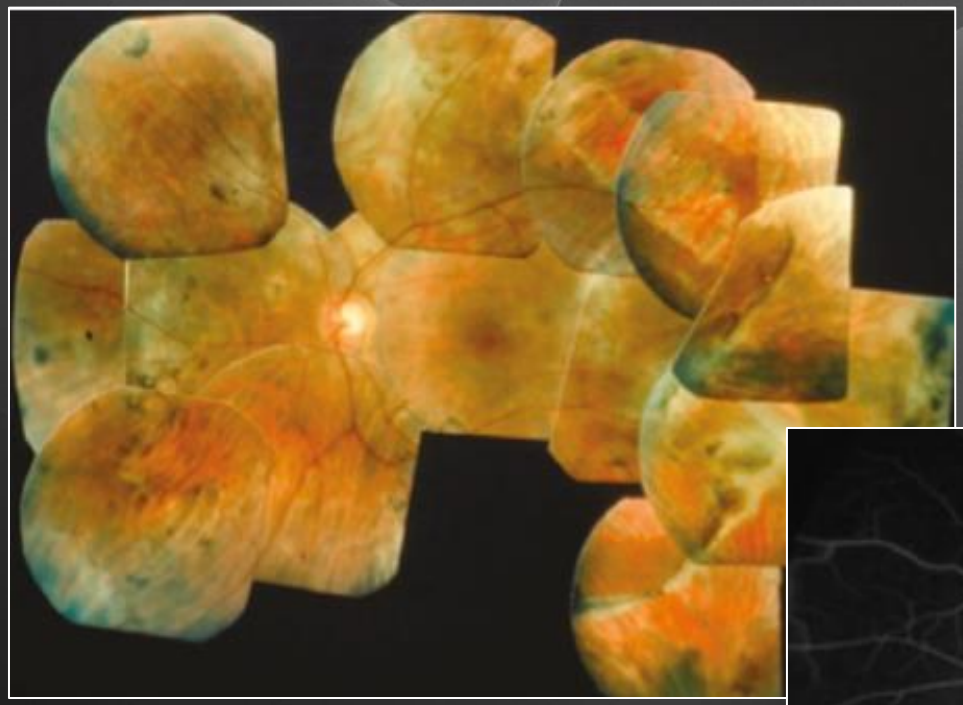

Intraoperative Imaging Technology

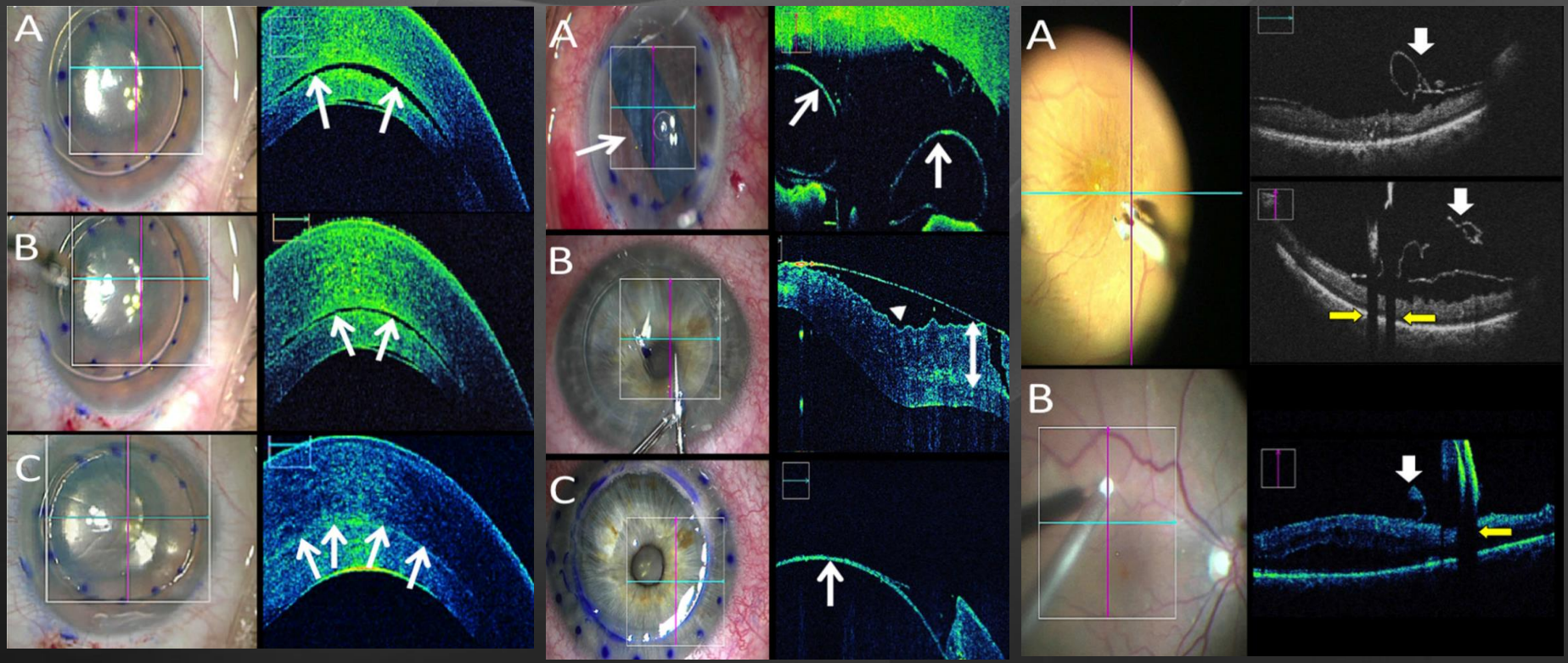

Strumentazioni Hi-Tech: che cosa?

- Aumento risoluzione e velocità di acquisizione
- Interpolazione dei dati
- Imaging multimediale: funzione e morfologia

  – OCT Swept Source
  – Angio OCT
  – Corneal imaging
  – Studio componente neuronale

Quali patologie?

- **Glaucoma**
  - **comprehensive analysis**
    - **optic nerve head**
    - **retinal nerve fiber layer**
    - **ganglion cell layer**

precisely matching unique scan patterns to the fine anatomical structures relevant

in glaucoma diagnostics

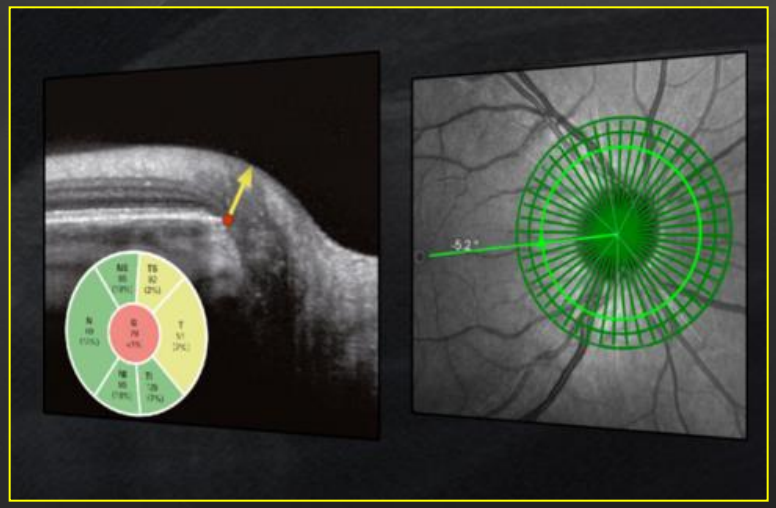

- **Retina**
  - **MultiColor Scanning Laser Imaging**
    - laser wavelengths simultaneously
    - distinct structures at different depths within the retina
    - structures and pathology not visible on ophthalmoscopy and fundus photography.
    - can even be acquired in patients with cataracts or nystagmus.

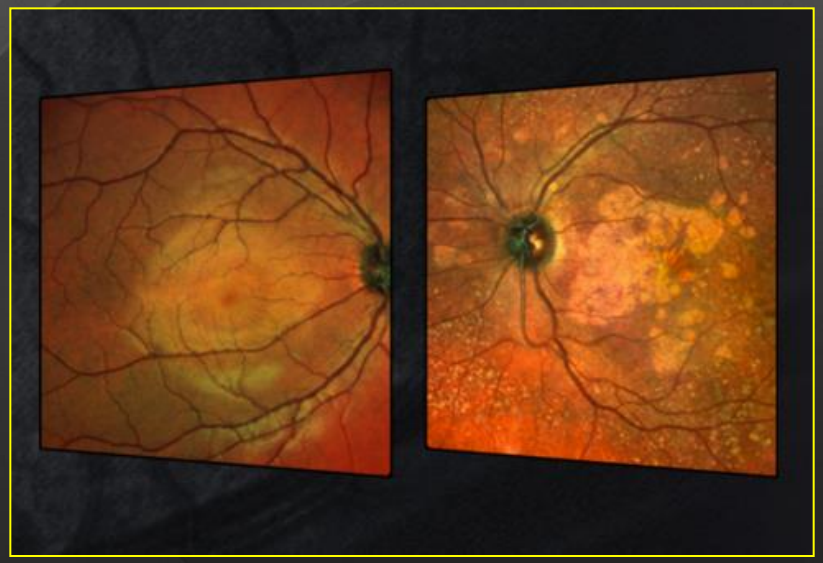

- **BluePeak**
  - scanning laser fundus imaging
  - a map of metabolic stress in the retina using lipofuscin as an indicator
  - RPE and photoreceptor cell malfunctions

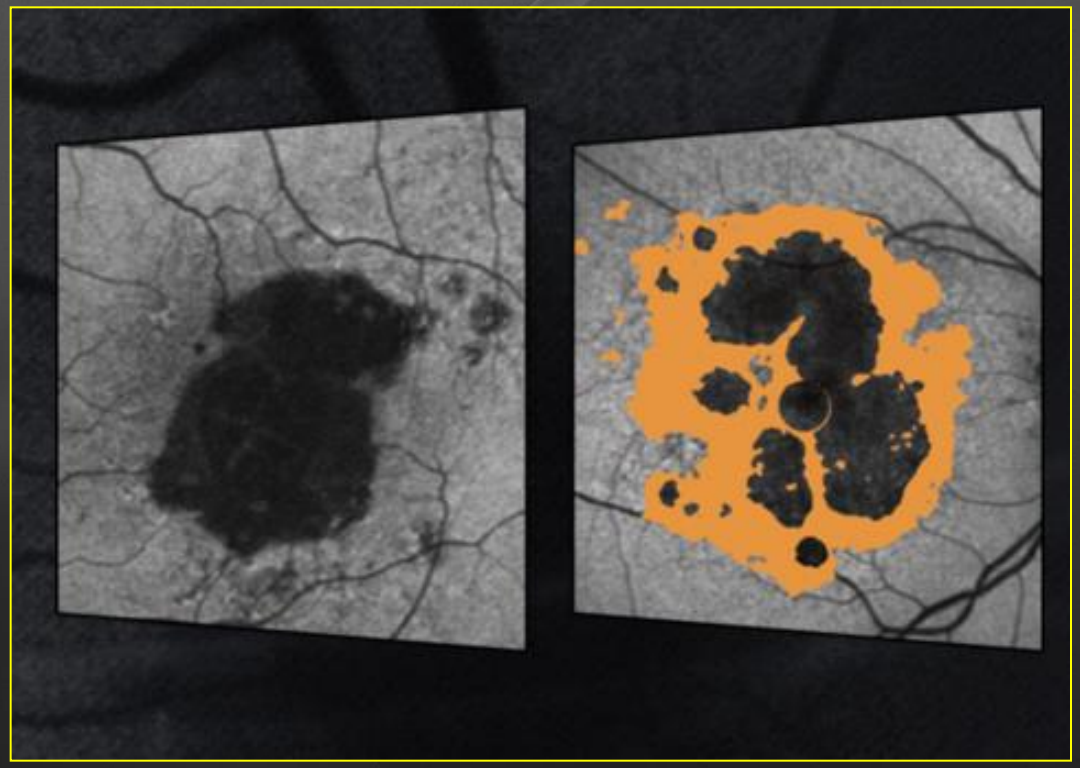

Cornea

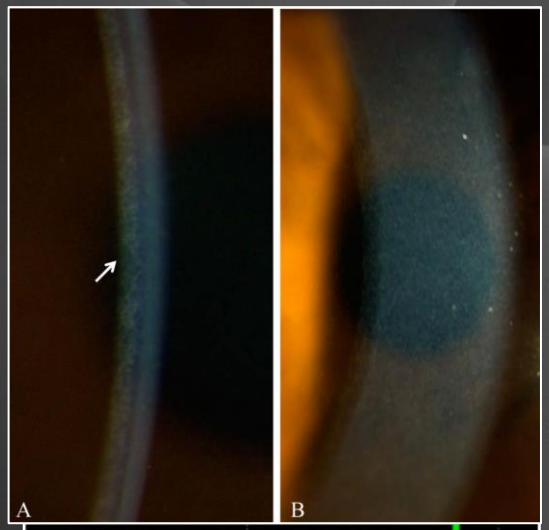
A
B

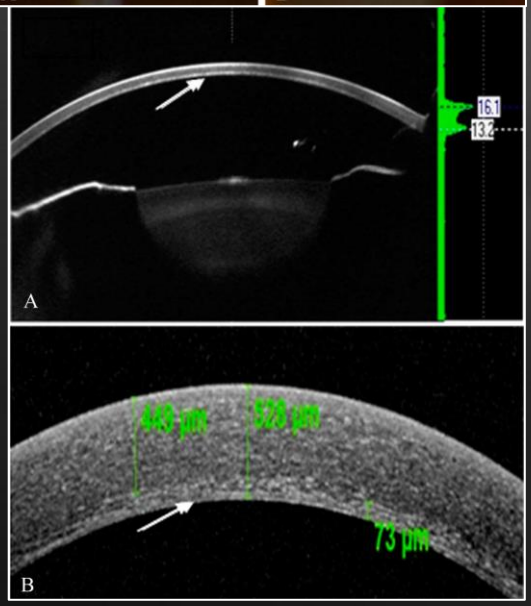
16.1
13.2
A
448 µm
573 µm
73 µm
B

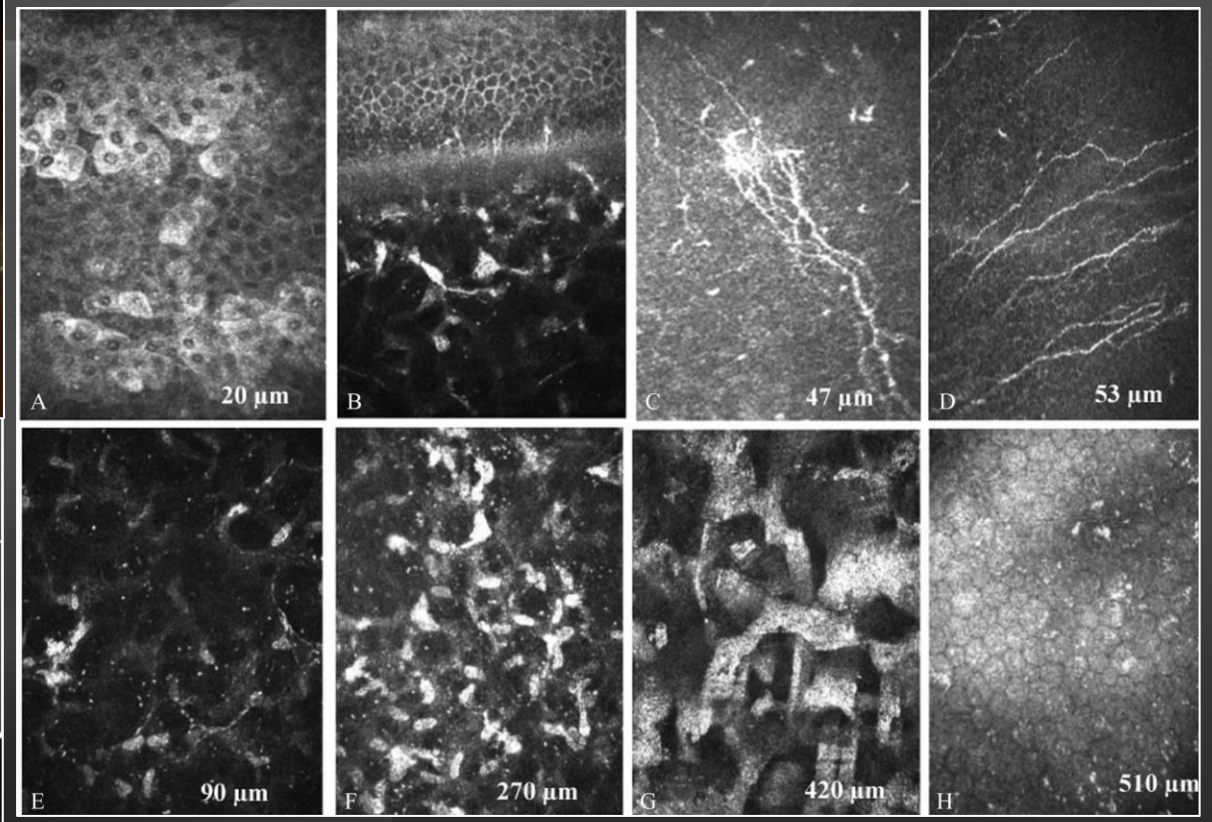
A
20 µm
B
C
47 µm
D
53 µm
E
90 µm
F
270 µm
G
420 µm
H
510 µm

Come lavorano?

- Acquisizione ad alta velocità
- Ottimizzazione del segnale (image averaging)
- Eye tracking multiplanare
- Eliminazione artefatti
- Elaborazione del segnale (scala di grigi o colore)

AN AUTOMATIC, INTERCAPILLARY AREA-BASED ALGORITHM FOR QUANTIFYING DIABETES-RELATED CAPILLARY DROPOUT USING OPTICAL COHERENCE TOMOGRAPHY ANGIOGRAPHY

JULIA SCHOTTENHAMML, BSc,*† ERIC M. MOULT, BSc,† STEFAN PLONER, BSc,*† BYUNGKUN LEE, MEng,† EDUARDO A. NOVAIS, MD,‡§ EMILY COLE, BSc,‡ SABIN DANG, MD,‡ CHEN D. LU, MSc,† LENNART HUSVOGT, BSc,* NADIA K. WAHEED, MD, MPH,‡ JAY S. DUKER, MD,‡ JOACHIM HORNEGGER, PhD,* JAMES G. FUJIMOTO, PhD†

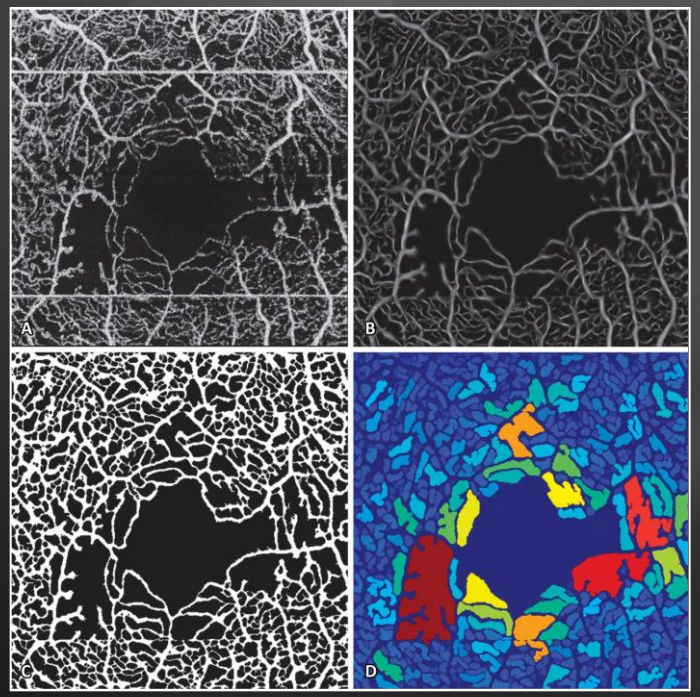

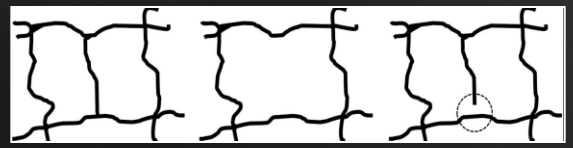

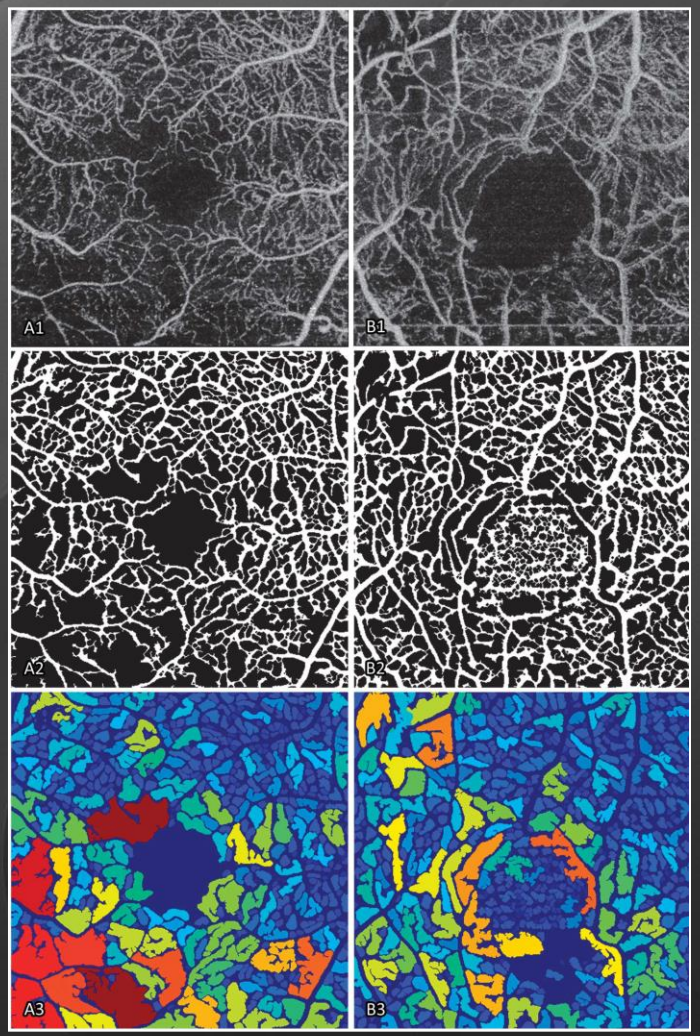

Automated volumetric segmentation of retinal fluid on optical coherence tomography

Jie Wang,[1,2] Miao Zhang,[1] Alex D. Pechauer,[1] Liang Liu,[1] Thomas S. Hwang,[1] David J. Wilson,[1] Dengwang Li,[2,*] and Yali Jia[1,*]

[1]Casey Eye Institute, Oregon Health & Science University, Portland, OR 97239, USA
[2]Shandong Province Key Laboratory of Medical Physics and Image Processing Technology, Shandong Normal University, Jinan, 250014, China
[*]jiaya@ohsu.edu

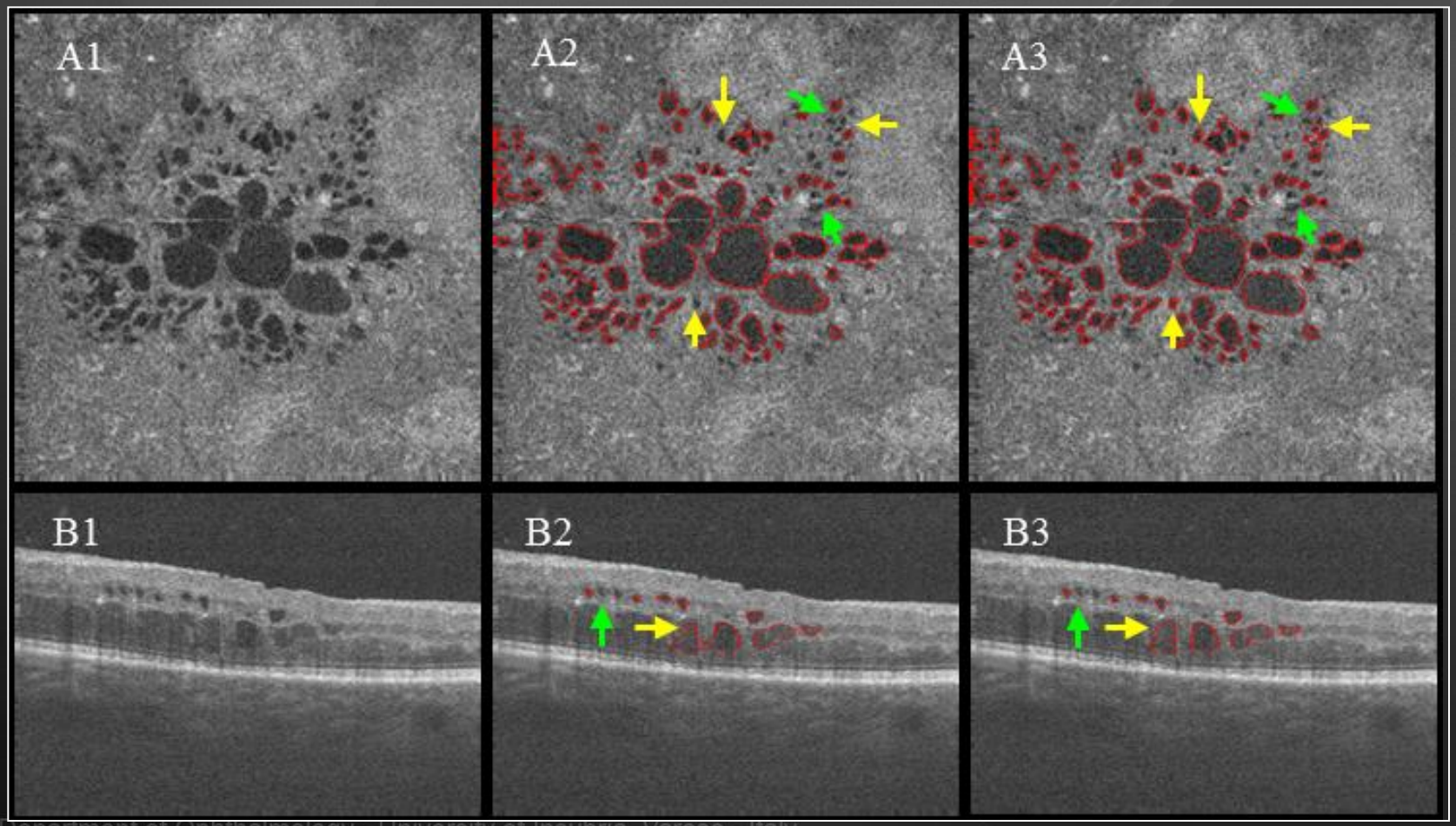

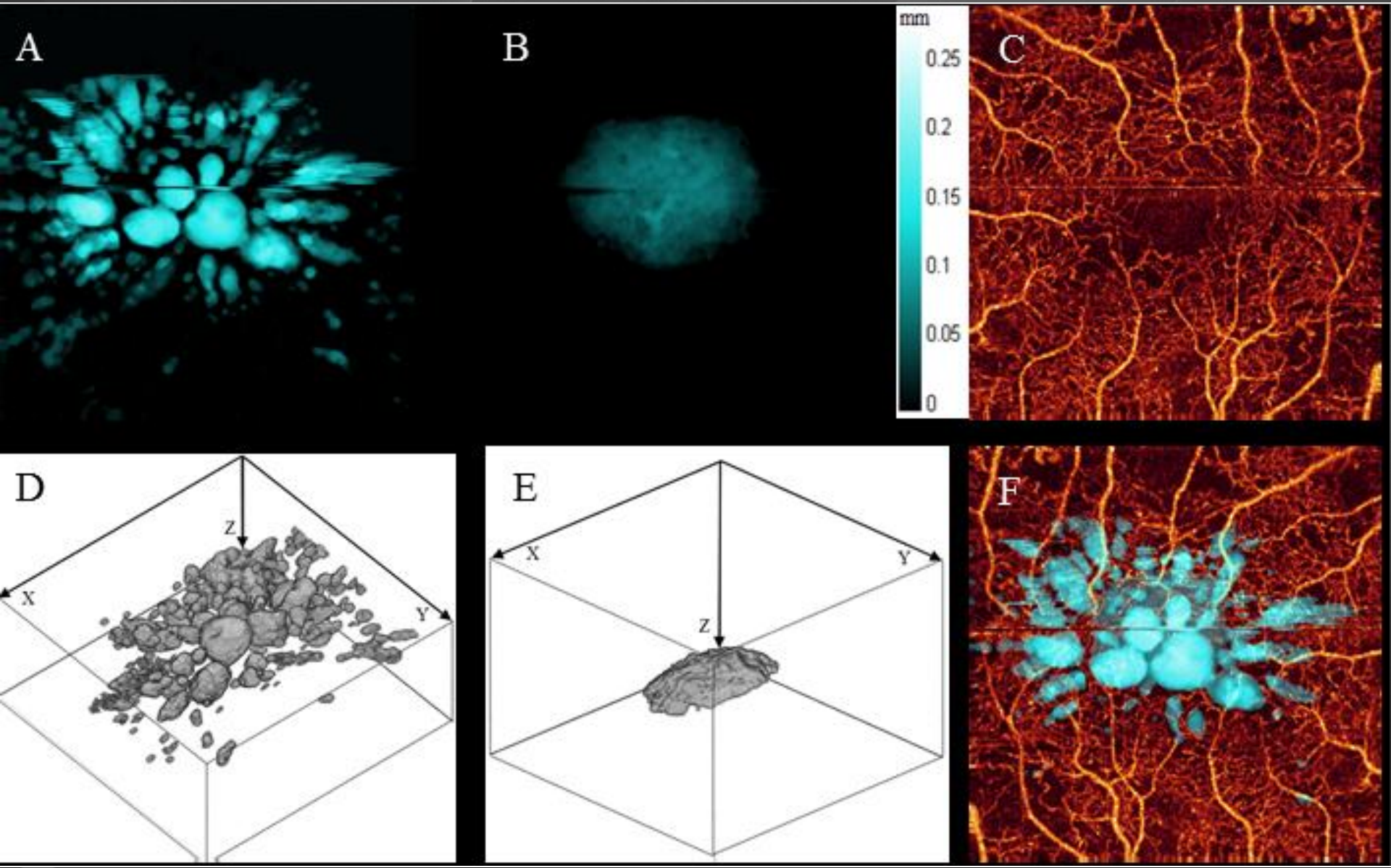
A
B
mm
0.25
0.2
0.15
0.1
0.05
0
C
D
Z
X
Y
E
X
Y
Z
F

Graefes Arch Clin Exp Ophthalmol (2016) 254:1661–1668
DOI 10.1007/s00417-016-3361-7

REVIEW ARTICLE

Multimodal retinal imaging of diabetic macular edema: toward new paradigms of pathophysiology

Edoardo Midena[1,2] · Silvia Bini[1]

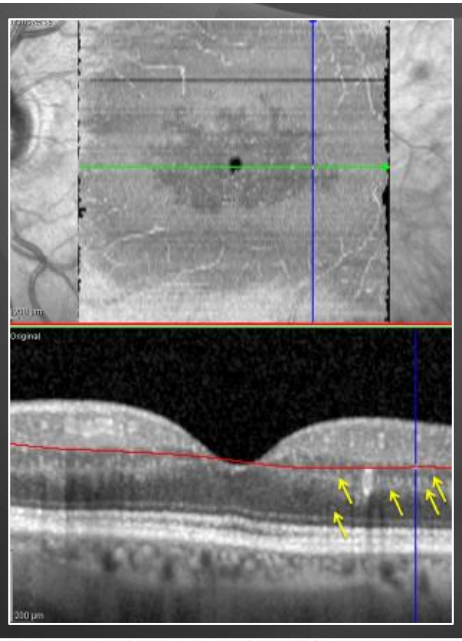

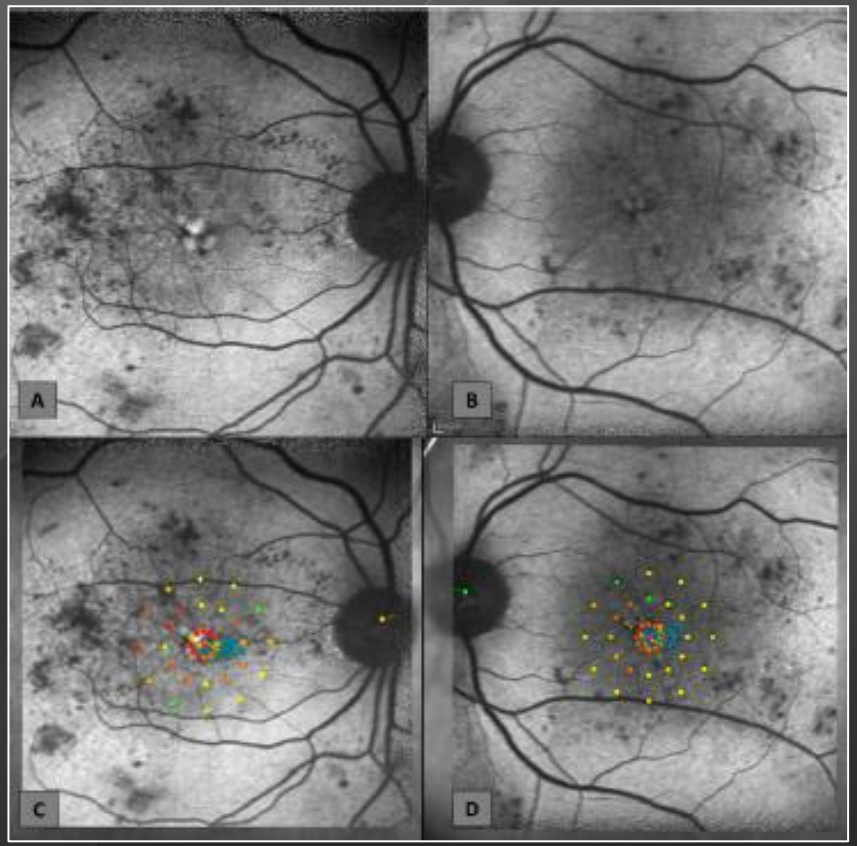

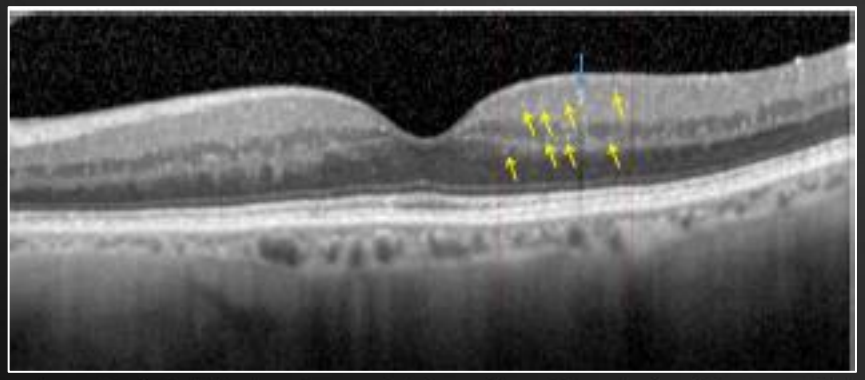

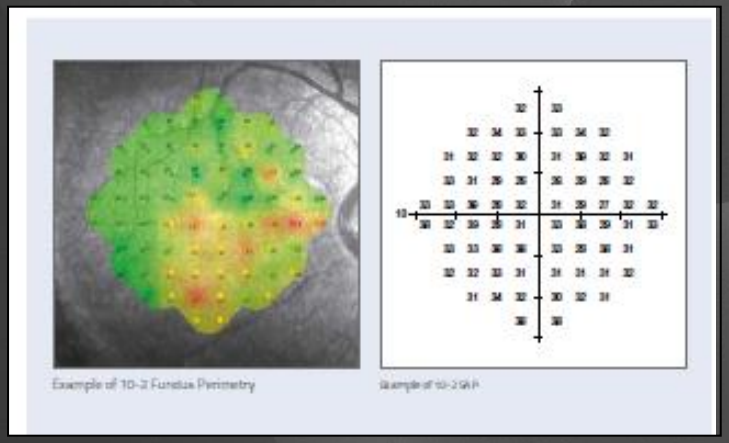
Example of 10-2 Fundus Perimetry

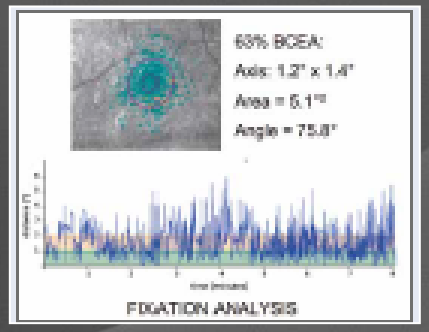
63% BCEA:
Axis: 1.2° x 1.4°
Area = 5.1°²
Angle = 75.8°
FIXATION ANALYSIS

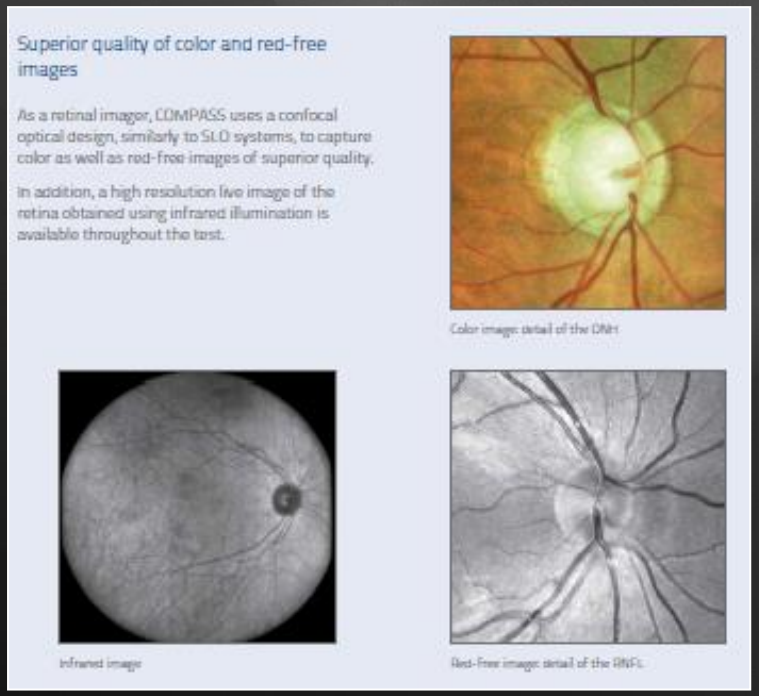
Superior quality of color and red-free images
As a retinal imager, COMPASS uses a confocal optical design, similarly to SLO systems, to capture color as well as red-free images of superior quality.
In addition, a high resolution live image of the retina obtained using infrared illumination is available throughout the test.
Color image: detail of the ONH
Infrared image
Red-Free image: detail of the RNFL

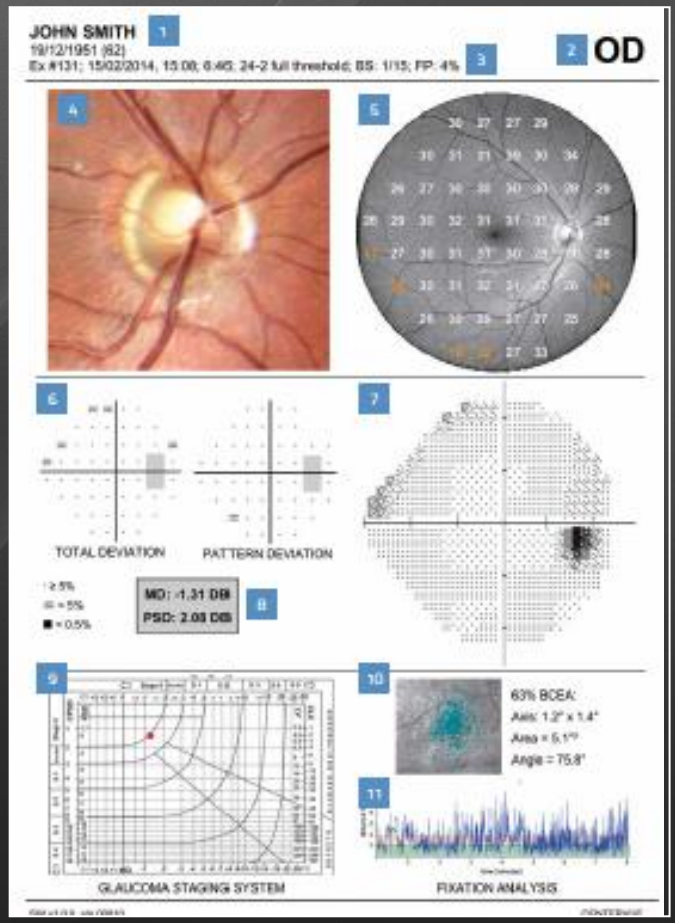
JOHN SMITH
19/12/1951 (62)
Ex #131; 15/02/2014, 15:08; 0.46; 24-2 full threshold; BS: 1/15; FP: 4%
OD
TOTAL DEVIATION
PATTERN DEVIATION
MD: -1.31 DB
PSD: 2.03 DB
63% BCEA:
Axis: 1.2° x 1.4°
Area = 5.1°²
Angle = 75.8°
GLAUCOMA STAGING SYSTEM
FIXATION ANALYSIS

Nuovi strumenti: nuovi problemi

- Validazione delle misure
- Database normativi
- Confronto tra strumenti
- Nuove strutture: che significato?

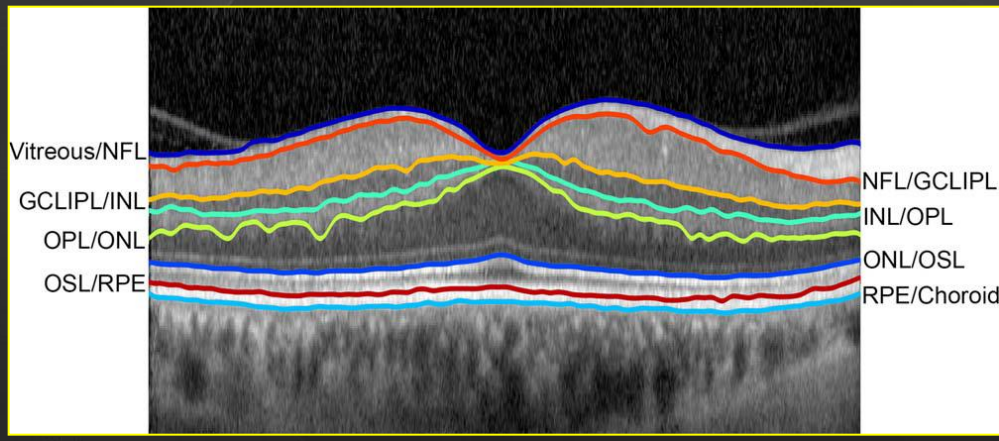

Normative Data for Vascular Density in Superficial and Deep Capillary Plexuses of Healthy Adults Assessed by Optical Coherence Tomography Angiography

Florence Coscas,[1] Alexandre Sellam,[1] Agnès Glacet-Bernard,[1] Camille Jung,[2] Mathilde Goudot,[1] Alexandra Miere,[1] and Eric H. Souied[1]

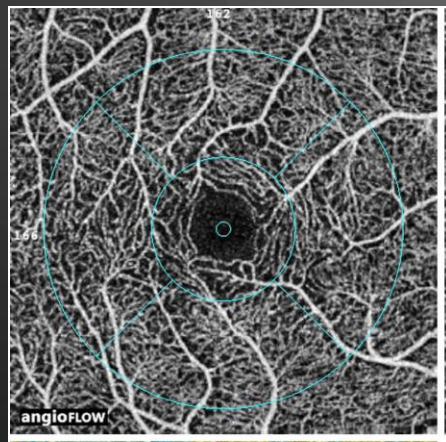

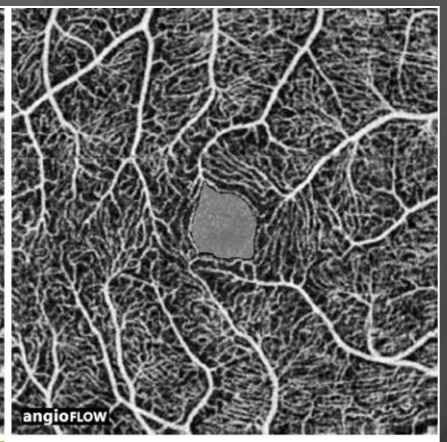

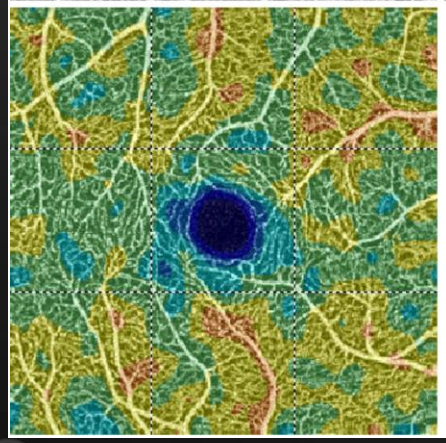

OCT Thickness ILM-RPE & Flow Density

Section	Thickness (µm)	Density (%)
Whole en face	N/A	54.20
Fovea	285	33.65
ParaFovea	332	56.01
- Tempo	321	52.95
- Superior	329	55.83
- Nasal	341	56.46
- Inferior	336	58.83

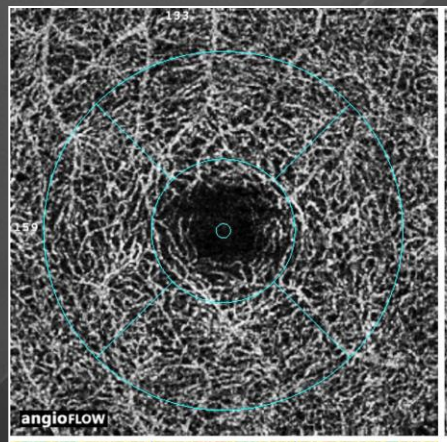

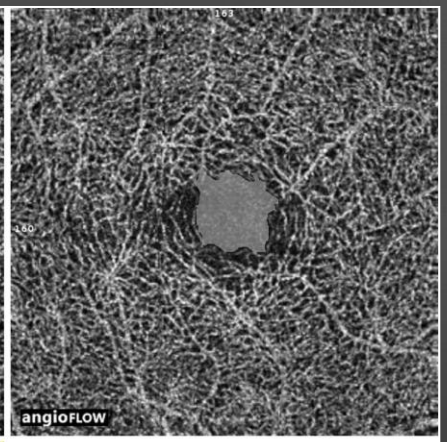

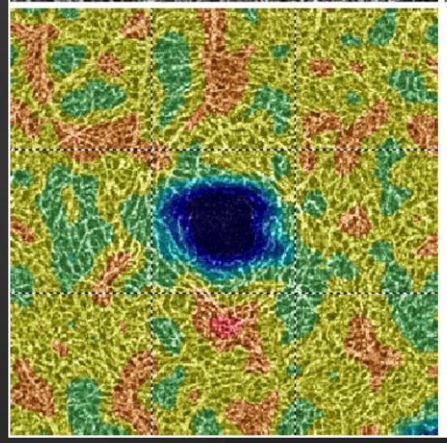

OCT Thickness ILM-RPE & Flow Density

Section	Thickness (µm)	Density (%)
Whole en face	N/A	58.54
Fovea	285	30.85
ParaFovea	332	61.00
- Tempo	321	58.90
- Superior	329	61.42
- Nasal	341	60.92
- Inferior	336	62.80

TABLE 7. Comparison of Superficial FAZ Area Using Different Imaging Modalities in Healthy Eyes According to Age

Authors	Technique/Algorithms	Diseased Subjects	Healthy Subjects' Eyes (Subjects)	Healthy Mean Age	Healthy Mean FAZ Area
Bresnick et al.,[33] 1984	Argentic FA	36	20	44 (24–52)	0.35 mm²
Arend et al.,[34] 1991	Scanning laser ophthalmoscope FA	48	21	26 ± 4	0.231 ± 0.06 mm²
Tam et al.,[30] 2010	Adaptive optics scanning laser ophthalmoscope	None	10	27 ± 6.4	0.323 ± 0.107 mm²
John et al.,[29] 2011	Contrast-adjusted scanning laser ophthalmoscope FA	None	31	29.7 (20–40)	0.275 ± 0.074 mm²
Kim et al.,[31] 2012	Phase-variance optical coherence tomography	8	2	54 (29–66)	<0.2 mm²
Chui et al.,[32] 2014	Adaptive optics scanning laser ophthalmoscope microangiography	No	32	Nd (22–61)	0.32 ± 0.16 mm²
De Carlo et al.,[17] 2015	OCT angiography ImageJ*	39	28 (22)	54 ± 11.61	0.348 (0.1085–0.671) mm²
Freiberg et al.,[26] 2015	OCT angiography ImageJ*	37	25 (22)	60.41 ± 20.35	0.661 ± 0.171, max vertical diameter
Kuehlewein et al.,[38] 2015	Swept-source OCT microangiography	None	19 (13)	31 ± 5 (26–41)	0.304 ± 0.132 mm²
Carpineto et al., [35] 2016	OCT angiography AngioAnalytics†	None	60 (60)	28.9 ± 7.6	0.251 ± 0.096 mm²
Samara et al.,[37] 2015	OCT angiography ImageJ*	None	67 (70)	42 (41, 12–76)	0.266 ± 0.097 mm²
Takase et al.,[36] 2015	OCT angiography ImageJ*	24	19 (Nd)	62.8 ± 11.3 (38–81)	0.25 ± 0.06 mm²
Coscas et al. (in our study), 2015	OCT angiography AngioAnalytics†	None	135 (70), 3 age groups	48.3 ± 17.5 (20–79)	0.28 ± 0.10 mm²

Multivendor Spectral-Domain Optical Coherence Tomography Dataset, Observer Annotation Performance Evaluation, and Standardized Evaluation Framework for Intraretinal Cystoid Fluid Segmentation

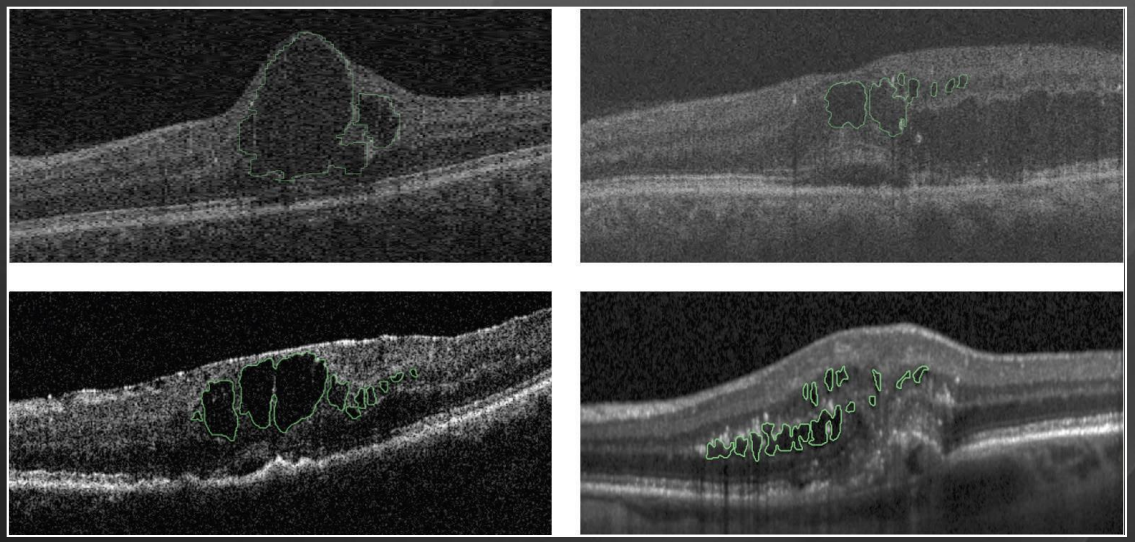

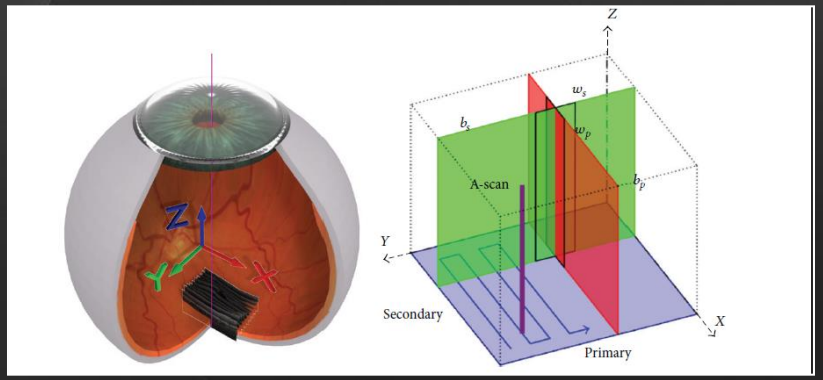

Automated Retinal Layer Segmentation Using Spectral Domain Optical Coherence Tomography: Evaluation of Inter-Session Repeatability and Agreement between Devices

Louise Terry[1], Nicola Cassels[1], Kelly Lu[1], Jennifer H. Acton[1], Tom H. Margrain[1], Rachel V. North[1], James Fergusson[1,2], Nick White[1,2], Ashley Wood[1]*

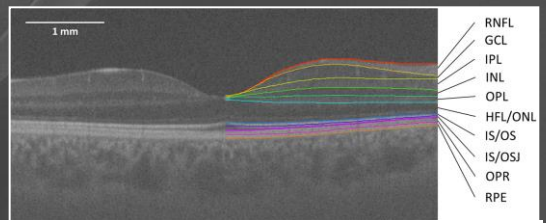

Table 1. Mean thickness of 10 intra-retinal layers. Thickness values (mean ± SD; μm) produced by segmentation of images at session 1 using the Iowa Reference Algorithms.

Layer	Fovea			Inner ring			Outer ring		
	Topcon	Zeiss	1040nm	Topcon	Zeiss	1040nm	Topcon	Zeiss	1040nm
1. RNFL	7.0 ± 2.3	5.9 ± 2.9	5.2 ± 2.2	25.5 ± 2.3	25.2 ± 2.3	24.2 ± 2.4	39.3 ± 7.0	40.9 ± 5.9	39.3 ± 5.0
2. GCL	17.0 ± 6.3	13.4 ± 5.4	17.2 ± 5.1	48.5 ± 5.9	52.4 ± 5.7	50.5 ± 6.2	24.7 ± 3.0	27.2 ± 3.1	29.3 ± 3.8
3. IPL	29.3 ± 2.9	27.5 ± 4.1	24.4 ± 4.2	42.5 ± 4.2	40.7 ± 3.5	39.9 ± 4.2	35.3 ± 2.8	37.3 ± 2.8	36.0 ± 3.8
4. INL	17.7 ± 4.6	22.5 ± 5.3	18.9 ± 4.2	37.8 ± 3.5	43.2 ± 3.8	37.5 ± 3.6	28.1 ± 3.3	32.9 ± 3.0	29.6 ± 3.3
5. OPL	23.0 ± 3.4	20.7 ± 4.9	20.3 ± 5.3	29.6 ± 3.8	28.0 ± 5.0	30.0 ± 5.1	26.2 ± 2.6	24.1 ± 3.0	28.4 ± 4.2
6. OPL-HFL ~BMEIS	120.8 ± 10.2	122.3 ± 9.2	116.5 ± 10.7	95.5 ± 8.8	96.9 ± 9.2	90.3 ± 8.8	79.7 ± 10.1	79.4 ± 6.4	71.6 ± 6.8
7. IS/OS	13.9 ± 0.9	11.7 ± 0.6	14.8 ± 2.4	12.6 ± 0.6	10.3 ± 0.4	13.7 ± 1.7	12.5 ± 1.2	10.2 ± 0.8	13.0 ± 1.7
8. IS/OSJ ~IB_OPR	17.0 ± 1.8	19.7 ± 2.2	17.3 ± 3.0	11.7 ± 1.4	14.0 ± 2.9	12.6 ± 2.4	10.3 ± 2.1	15.5 ± 4.3	15.8 ± 4.4
9. OPR	20.1 ± 2.6	20.7 ± 3.0	20.6 ± 3.8	19.8 ± 2.2	21.3 ± 3.3	20.7 ± 3.4	18.5 ± 2.3	17.8 ± 4.8	15.2 ± 3.8
10. RPE	18.6 ± 2.1	15.5 ± 0.5	15.6 ± 0.2	18.6 ± 1.7	15.5 ± 0.4	15.5 ± 0.2	18.6 ± 1.6	15.3 ± 0.5	15.5 ± 0.4

doi:10.1371/journal.pone.0162001.t001

Validation of Macular Choroidal Thickness Measurements from Automated SD-OCT Image Segmentation

Michael D. Twa*, Krystal L. Schulle†, Stephanie J. Chiu‡, Sina Farsiu‡, and David A. Berntsen*

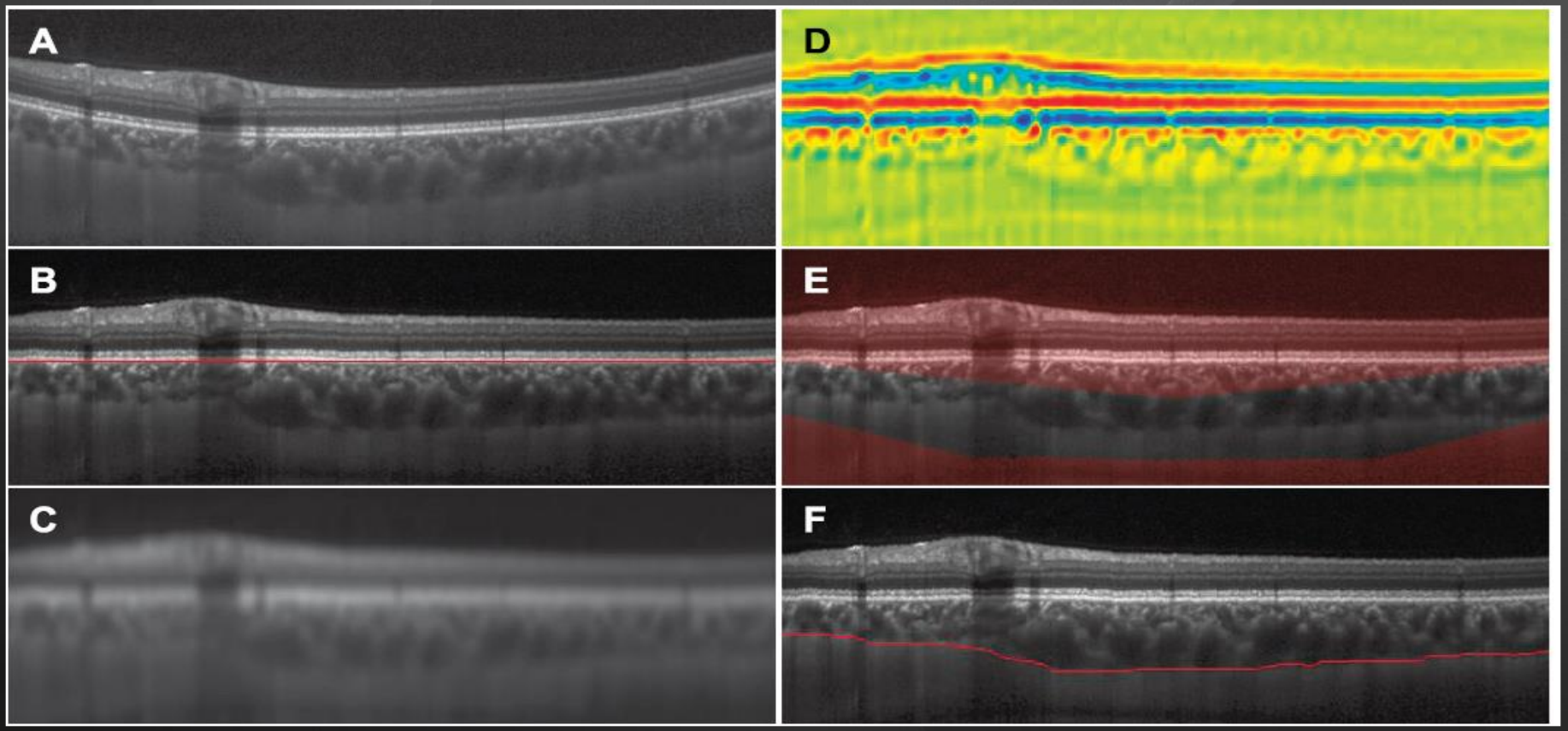

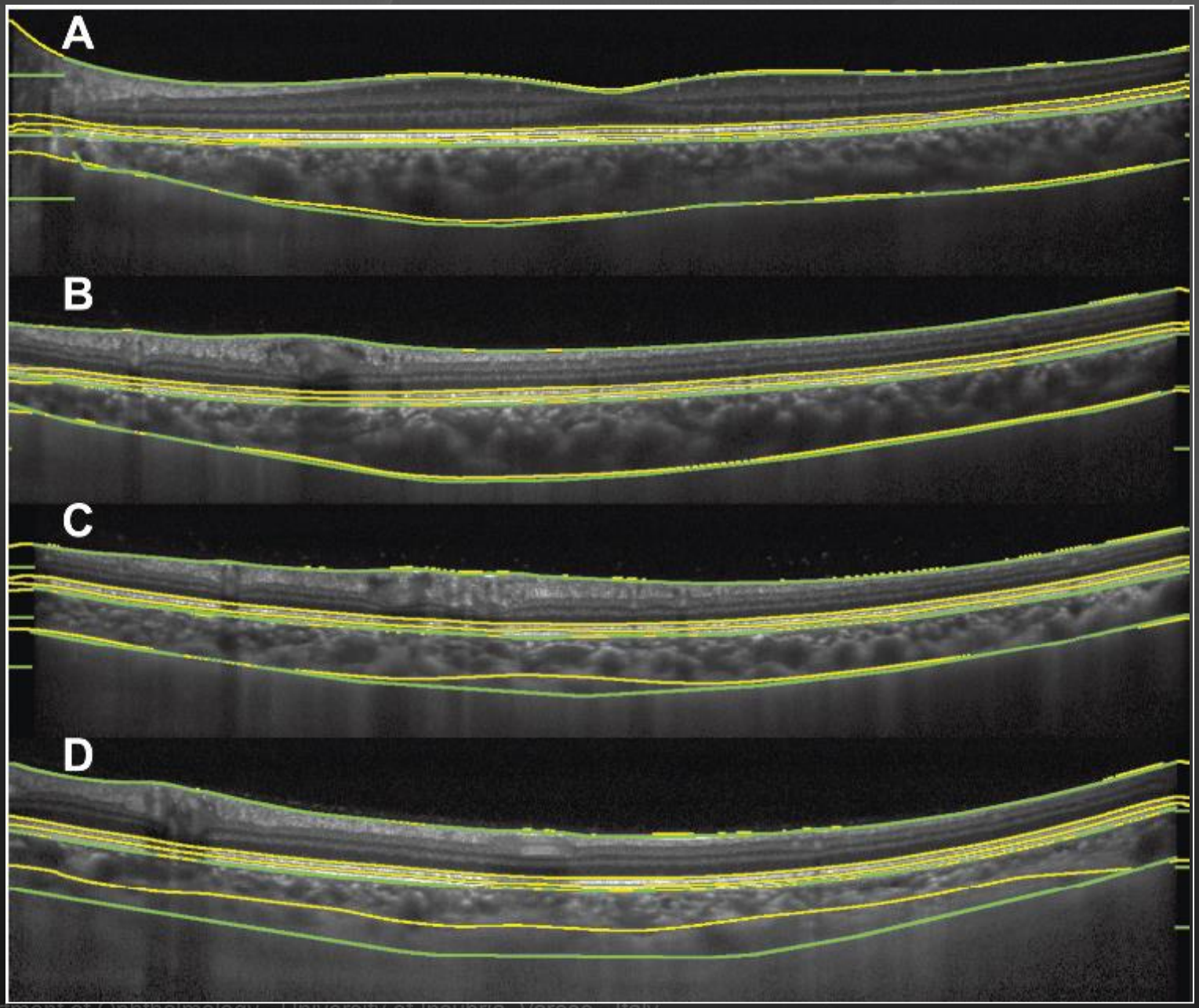
A
B
C
D

Drusen volume development over time and its relevance to the course of age-related macular degeneration

Ferdinand G Schlanitz,[1] Bernhard Baumann,[2] Michael Kundi,[3] Stefan Sacu,[1] Magdalena Baratsits,[1] Ulrike Scheschy,[1] Abtin Shahlaee,[1] Tamara J Mittermüller,[1] Alessio Montuoro,[1] Philipp Roberts,[1] Michael Pircher,[2] Christoph K Hitzenberger,[2] Ursula Schmidt-Erfurth[1]

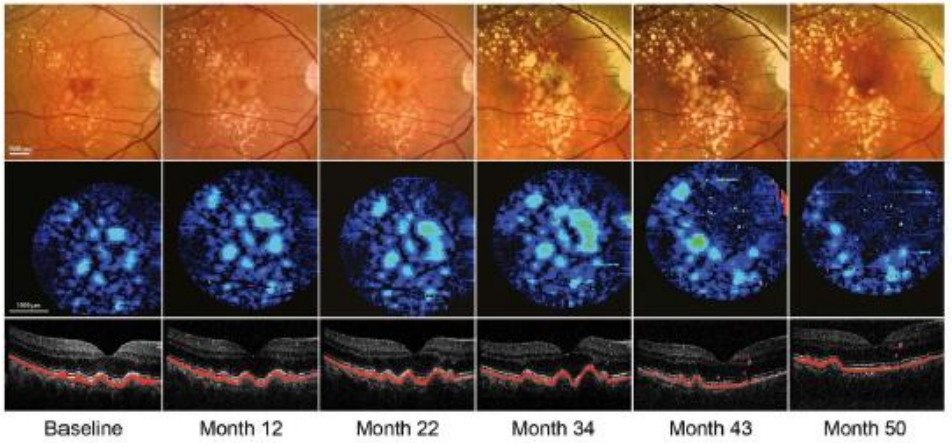

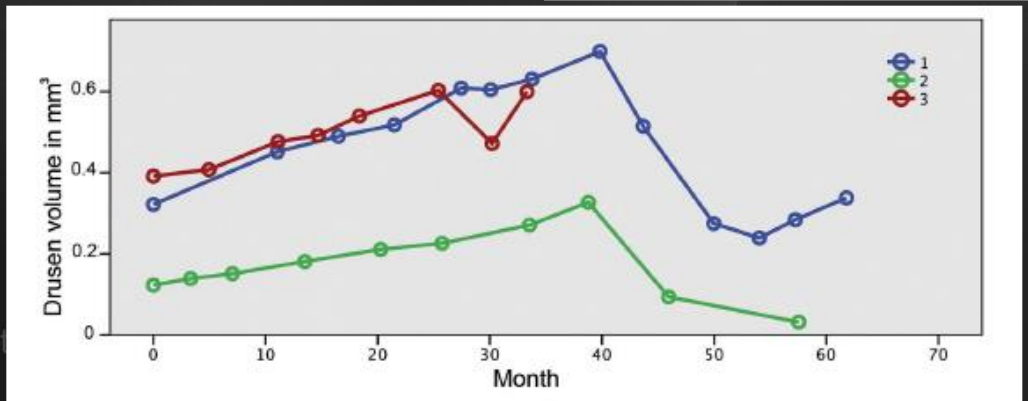

Alterations in Retinal Layer Thickness and Reflectance at Different Stages of Diabetic Retinopathy by En Face Optical Coherence Tomography

Justin Wanek, Norman P. Blair, Felix Y. Chau, Jennifer I. Lim, Yannek I. Leiderman, and Mahnaz Shahidi

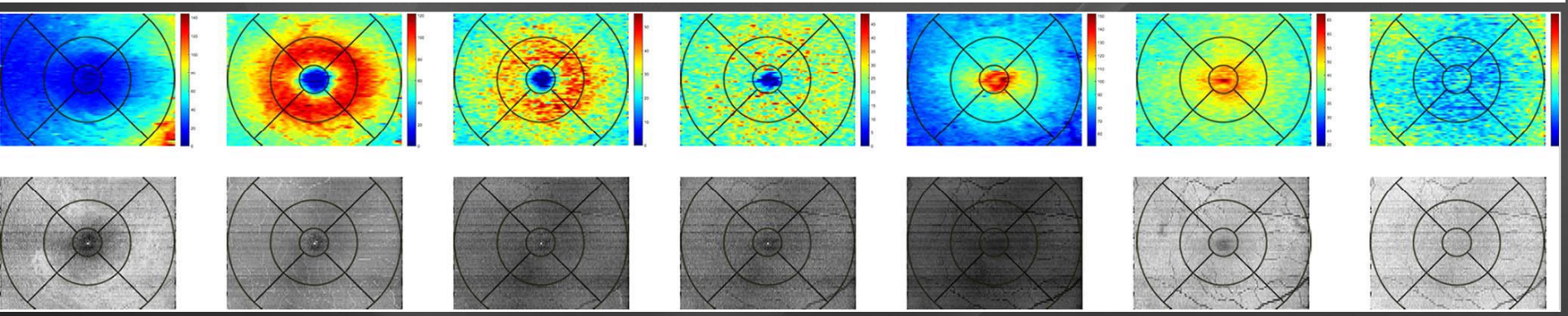

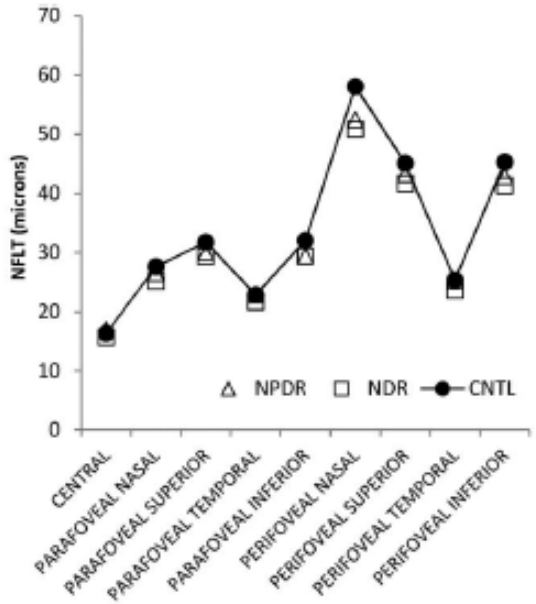
NFLT (microns)
70
60
50
40
30
20
10
0
NPDR
NDR
CNTL
CENTRAL
PARAFOVEAL NASAL
PARAFOVEAL SUPERIOR
PARAFOVEAL TEMPORAL
PARAFOVEAL INFERIOR
PERIFOVEAL NASAL
PERIFOVEAL SUPERIOR
PERIFOVEAL TEMPORAL
PERIFOVEAL INFERIOR

A

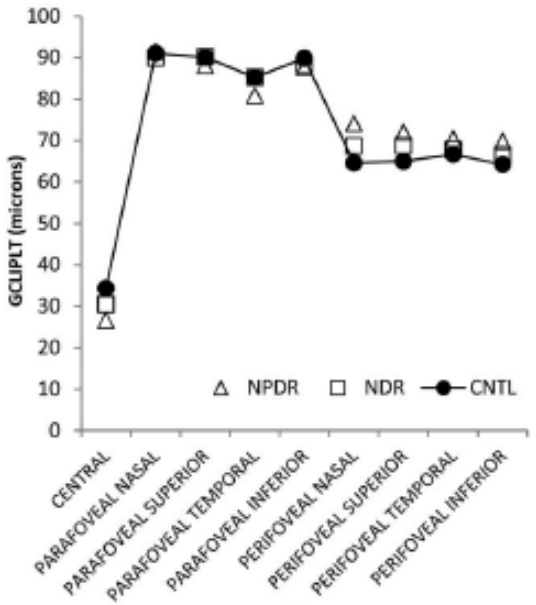
GCLIPLT (microns)
100
90
80
70
60
50
40
30
20
10
0
NPDR
NDR
CNTL
CENTRAL
PARAFOVEAL NASAL
PARAFOVEAL SUPERIOR
PARAFOVEAL TEMPORAL
PARAFOVEAL INFERIOR
PERIFOVEAL NASAL
PERIFOVEAL SUPERIOR
PERIFOVEAL TEMPORAL
PERIFOVEAL INFERIOR

B

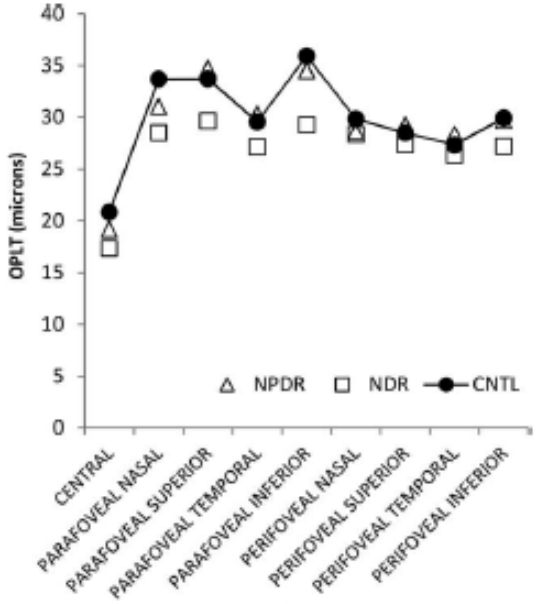
OPLT (microns)
40
35
30
25
20
15
10
5
0
NPDR
NDR
CNTL
CENTRAL
PARAFOVEAL NASAL
PARAFOVEAL SUPERIOR
PARAFOVEAL TEMPORAL
PARAFOVEAL INFERIOR
PERIFOVEAL NASAL
PERIFOVEAL SUPERIOR
PERIFOVEAL TEMPORAL
PERIFOVEAL INFERIOR

C

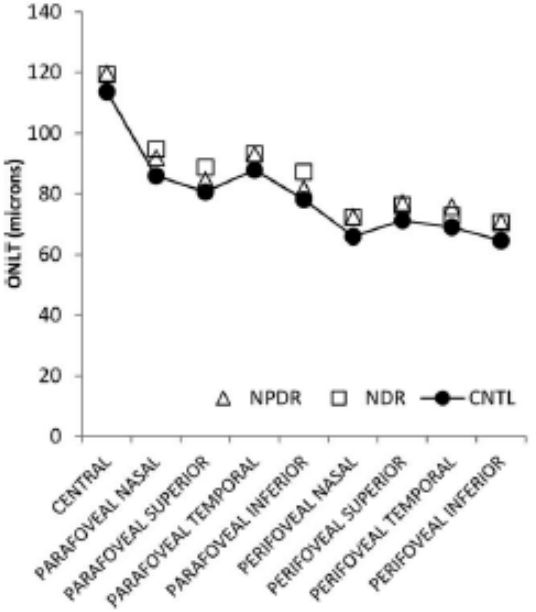
ONLT (microns)
140
120
100
80
60
40
20
0
NPDR
NDR
CNTL
CENTRAL
PARAFOVEAL NASAL
PARAFOVEAL SUPERIOR
PARAFOVEAL TEMPORAL
PARAFOVEAL INFERIOR
PERIFOVEAL NASAL
PERIFOVEAL SUPERIOR
PERIFOVEAL TEMPORAL
PERIFOVEAL INFERIOR

D

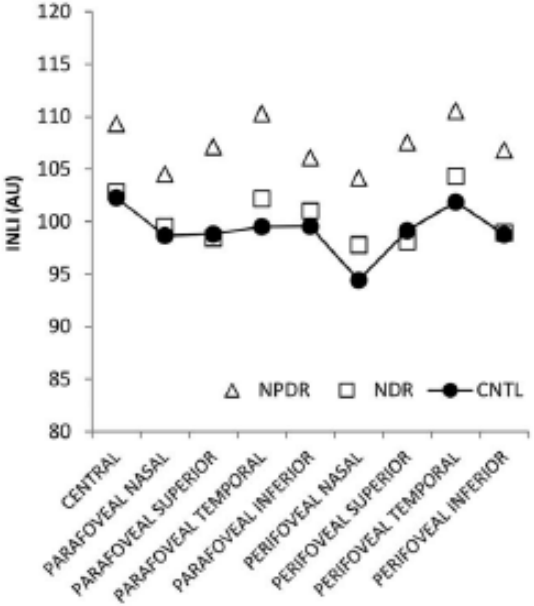
INLI (AU)
120
115
110
105
100
95
90
85
80
NPDR
NDR
CNTL
CENTRAL
PARAFOVEAL NASAL
PARAFOVEAL SUPERIOR
PARAFOVEAL TEMPORAL
PARAFOVEAL INFERIOR
PERIFOVEAL NASAL
PERIFOVEAL SUPERIOR
PERIFOVEAL TEMPORAL
PERIFOVEAL INFERIOR

E

Comparative Assessment for the Ability of Cirrus, RTVue, and 3D-OCT to Diagnose Glaucoma

Azusa Akashi, Akiyasu Kanamori, Makoto Nakamura, Masashi Fujihara, Yuko Yamada, and Akira Negi

TABLE 1. Scan Parameters for Cirrus, RTVue, and 3D-OCT

	Cirrus	RTVue	3D OCT-2000
Scan speed, 1 scan per second	27,000	26,000	50,000
Software version	6.1.0.96	4.0.5.39	8.00
Scan program of cpRNFL thickness	Optic Disc cube 200 × 200	3D disc & ONH	3D disc
Obtained data of cpRNFL thickness	256 points	16 sectors	1,024 points
Scan program of macular	Macular cube 200 × 200	GCC	3D macular
Analyzed macular area	4 × 4.8 mm, oval	6 × 6 mm, circle	6 × 6 mm, square
Obtained macular parameters	GCC, mRNFL, GCL/IPL	GCC	GCC, mRNFL, GCL/IPL
Obtained sectors of macular area	6 sectors	Superior/inferior	10 × 10 grids

TABLE 3. Area Under the ROC Curve Analysis Using Cirrus, RTVue, and 3D-OCT for All-Stage Glaucomatous Eyes (Means ± SE)

	SD-OCT Instruments (±SD)			*P* Value		
Measured Thickness Parameters	Cirrus	RTVue	3D-OCT	Cirrus vs. RTVue	RTVue vs. 3D-OCT	Cirrus vs. 3D-OCT
CpRNFL						
Average	0.964 (±0.011)	0.968 (±0.010)	0.957 (±0.013)	0.50	0.28	0.44
Superior	0.906 (±0.021)	0.912 (±0.020)	0.909 (±0.021)	0.59	0.85	0.79
Temporal	0.828 (±0.030)	0.857 (±0.028)	0.800 (±0.033)	0.07	0.008*	0.14
Inferior	0.952 (±0.013)	0.947 (±0.015)	0.955 (±0.013)	0.54	0.46	0.75
Nasal	0.686 (±0.043)	0.763 (±0.037)	0.689 (±0.019)	0.02*	0.019*	0.94
GCC						
Average	0.914 (±0.021)	0.932 (±0.018)	0.919 (±0.019)	0.05	0.30	0.25
Superior	0.803 (±0.033)	0.867 (±0.026)	0.813 (±0.025)	<0.001*	0.04*	0.55
Inferior	0.908 (±0.020)	0.925 (±0.018)	0.901 (±0.022)	0.098	0.066	0.62
GCL/IPL						
Average	0.888 (±0.032)	N.A.	0.830 (±0.032)			0.009*
Superior	0.804 (±0.033)	N.A.	0.763 (±0.039)			0.059
Inferior	0.908 (±0.022)	N.A.	0.856 (±0.028)			0.009*
mRNFL						
Average	0.868 (±0.026)	N.A.	0.931 (±0.019)			0.002*
Superior	0.742 (±0.040)	N.A.	0.931 (±0.028)			<0.001*
Inferior	0.877 (±0.025)	N.A.	0.919 (±0.020)			0.024*

N.A., not applicable.
* $P < 0.05$.

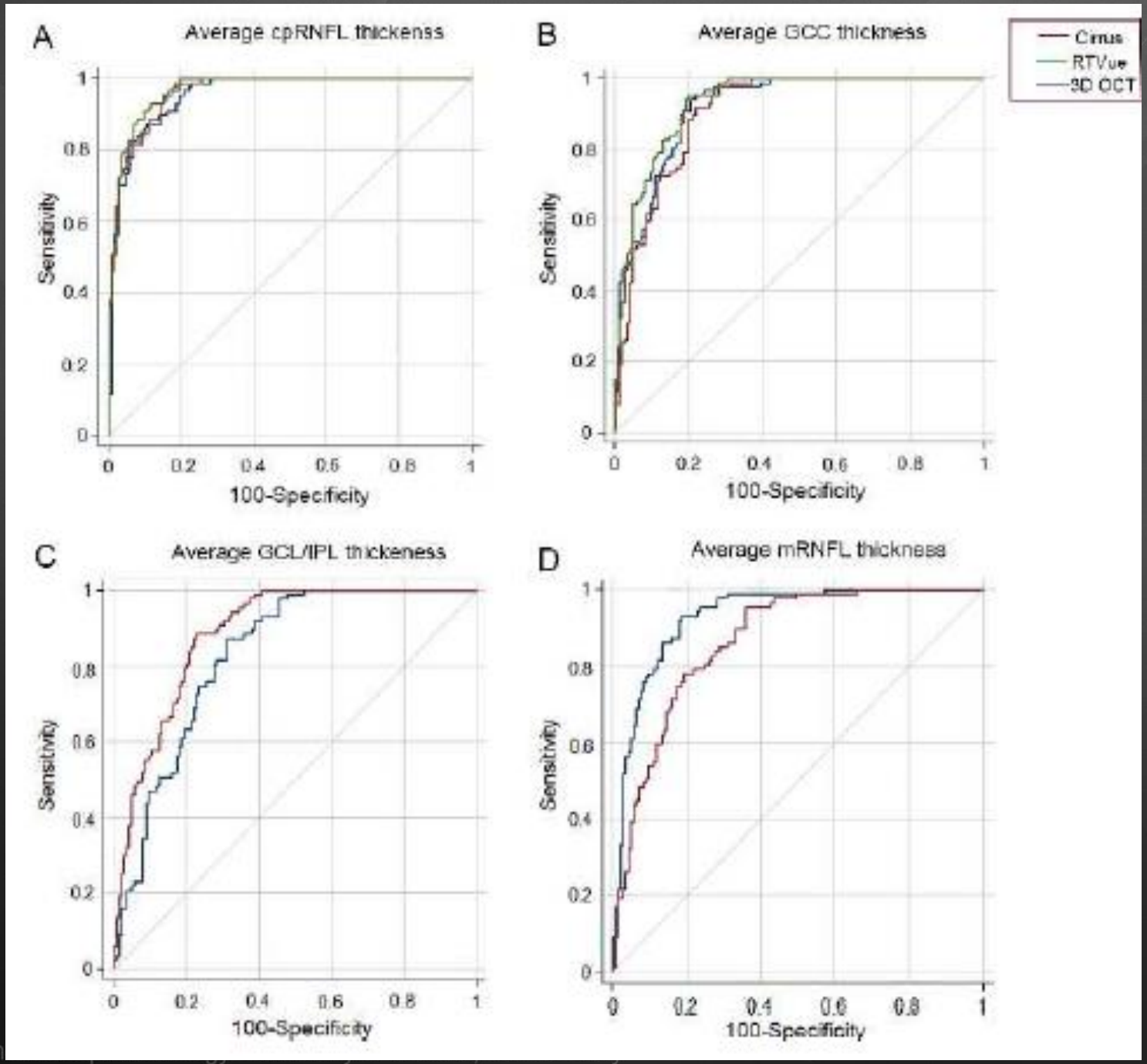
A
Average cpRNFL thickness
Sensitivity
100-Specificity
B
Average GCC thickness
Sensitivity
100-Specificity
Cirrus
RTVue
3D OCT
C
Average GCL/IPL thickness
Sensitivity
100-Specificity
D
Average mRNFL thickness
Sensitivity
100-Specificity

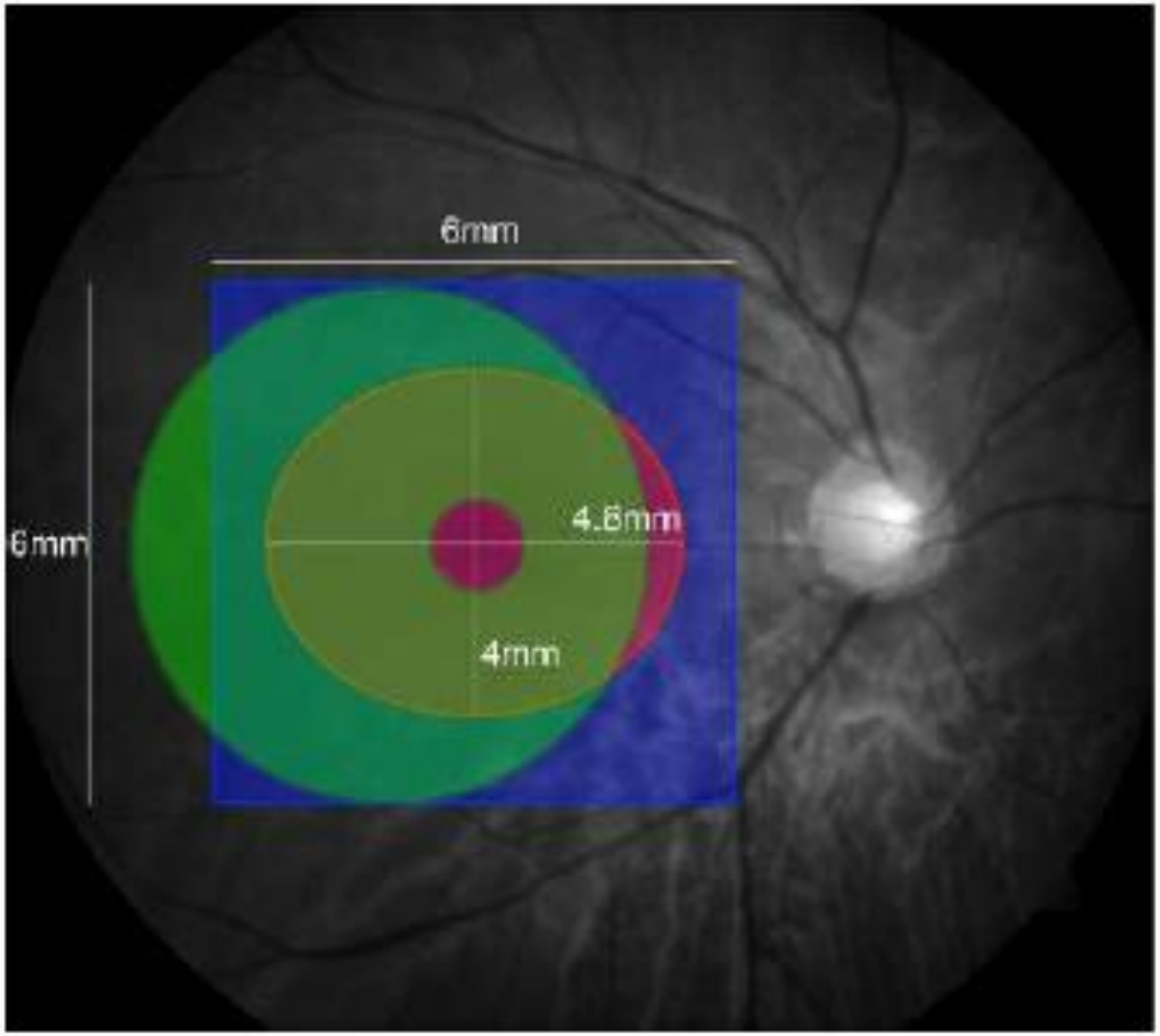

Cirrus

3D-OCT

RTVue

Glaucoma Diagnostic Ability of Layer-by-Layer Segmented Ganglion Cell Complex by Spectral-Domain Optical Coherence Tomography

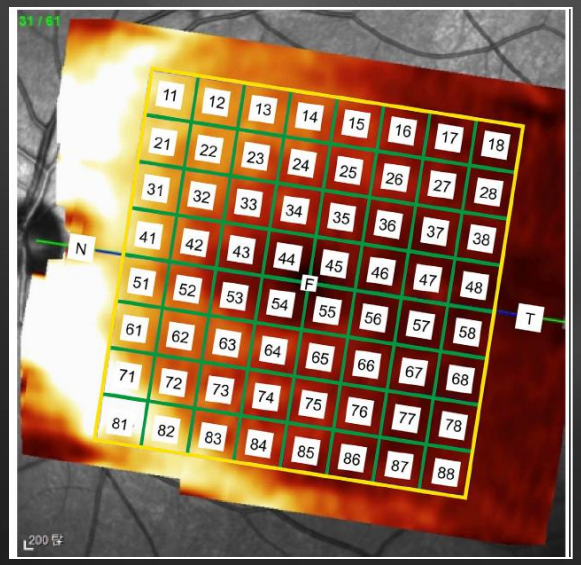

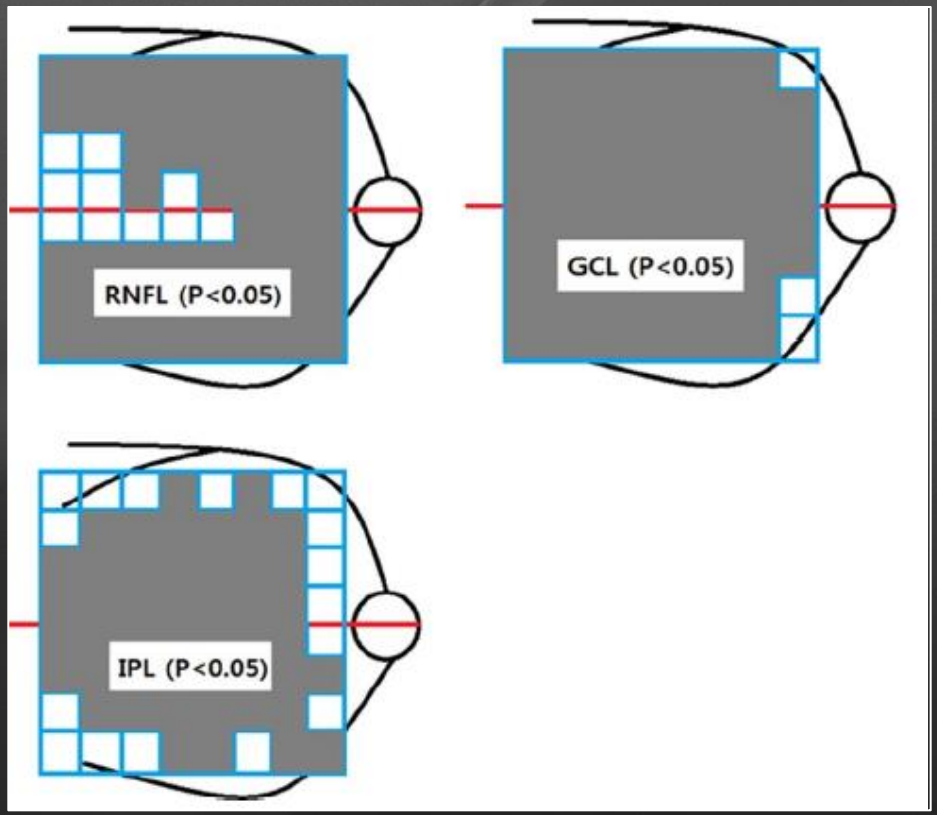

Comparison of Two Different OCT Systems: Retina Layer Segmentation and Impact on Structure-Function Analysis in Glaucoma

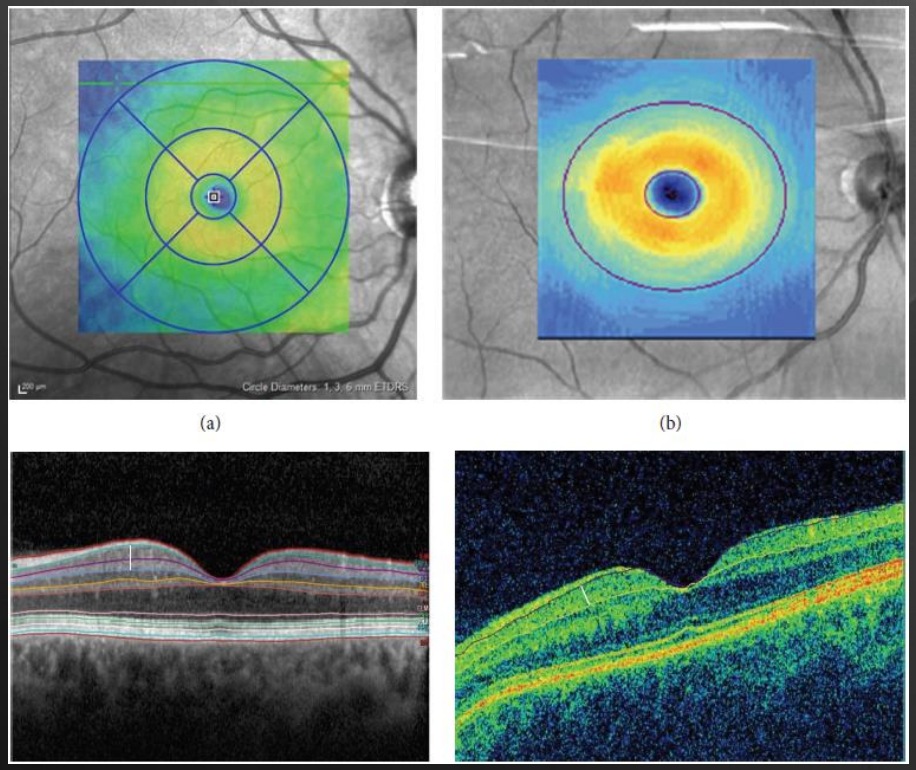

(a) (b)

Table 3: Total macula and ganglion cell layer mean thickness, in micrometers (μm), among groups and p values in the central 10°.

	POAG	Controls	p value*	AUC
	MT (mean ± SD)			
Cirrus				
MT	297.6 ± 13.5	307.9 ± 12.1	**0.036**	0.789
Spectralis				
MT	319.0 ± 13.0	329.8 ± 11.7	**0.027**	0.801
cMT	319.0 ± 12.9	329.8 ± 11.7	**0.027**	0.805
	GCIPL (mean ± SD)			
Cirrus				
GCIPL	68.5 ± 8.7	80.7 ± 4.7	**<0.01**	0.879
mGCIPL	61.2 ± 10.8	79.5 ± 4.7	**<0.01**	0.930
Spectralis				
GCIPL	75.7 ± 13.8	93.3 ± 4.6	**<0.01**	0.886
cGCIPL	76.1 ± 13.7	93.4 ± 4.6	**<0.01**	0.886

MT: full macular thickness, GCIPL: ganglion cell-inner plexiform layer thickness, cMT and cGCIPL: average values after manual correction of layer segmentation in Spectralis OCT, mGCIPL: minimum GCIPL value calculated by Cirrus software. AUC: area under the ROC curve. SD: standard deviation. * p values were obtained with paired t-test and posterior adjustment with FDR (false discovery rate).

Macular SD-OCT Outcome Measures: Comparison of Local Structure-Function Relationships and Dynamic Range

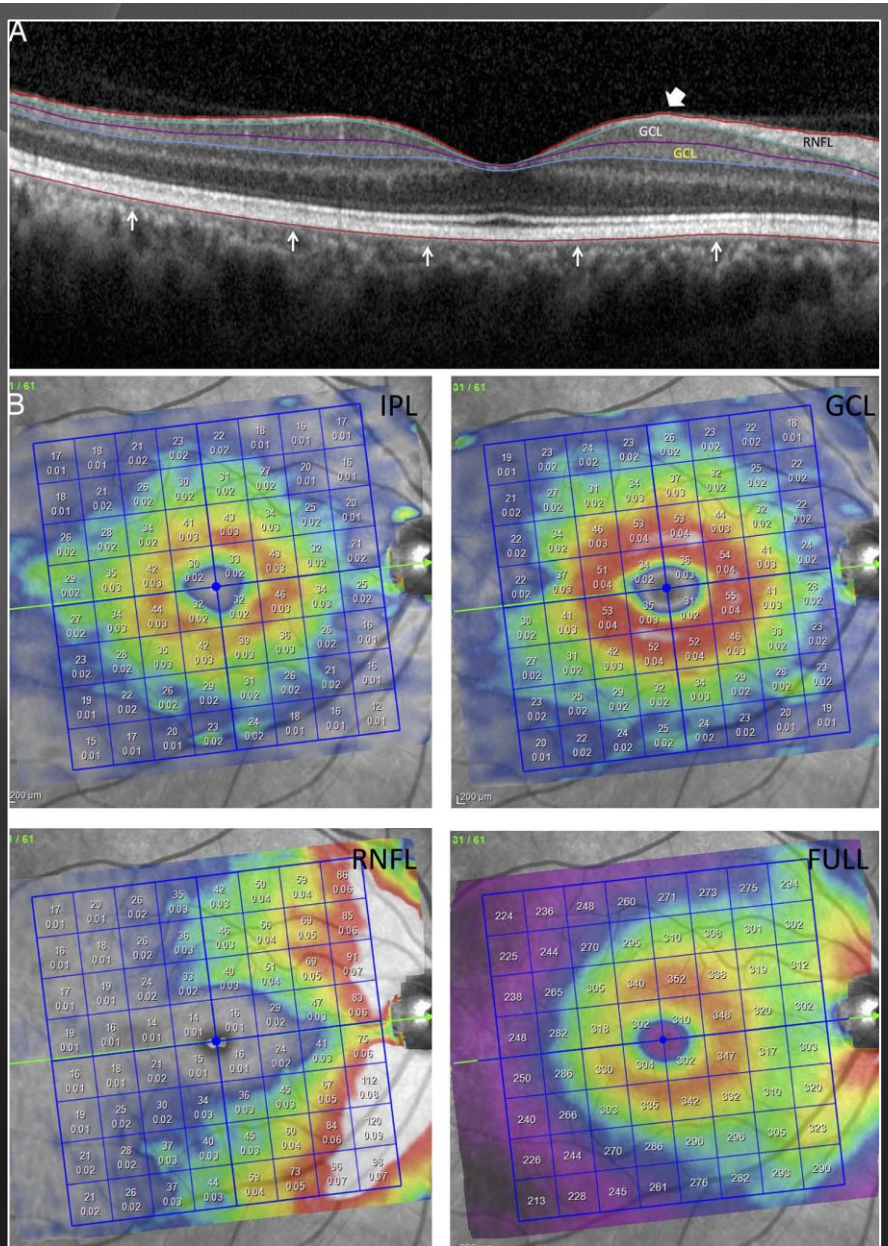

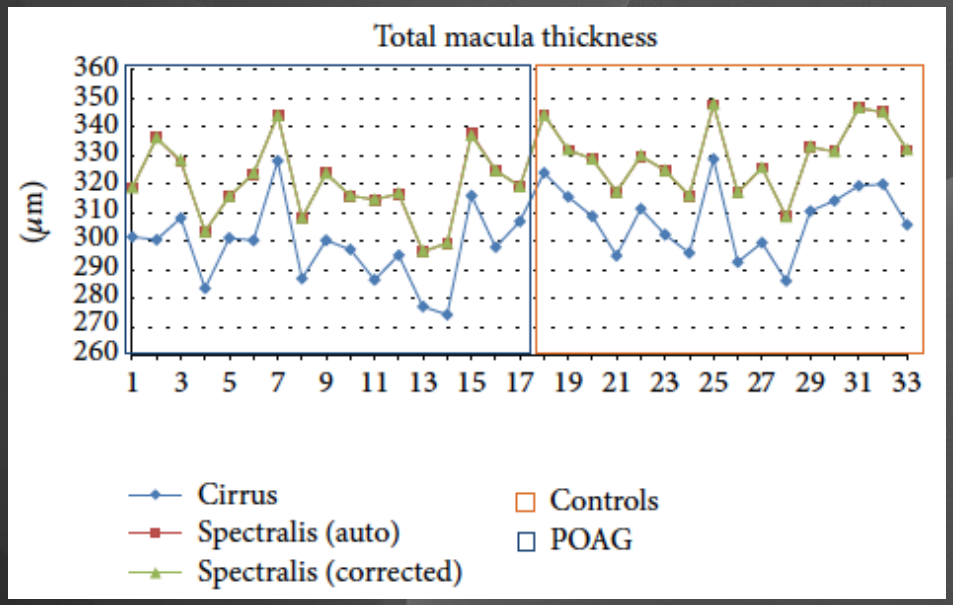

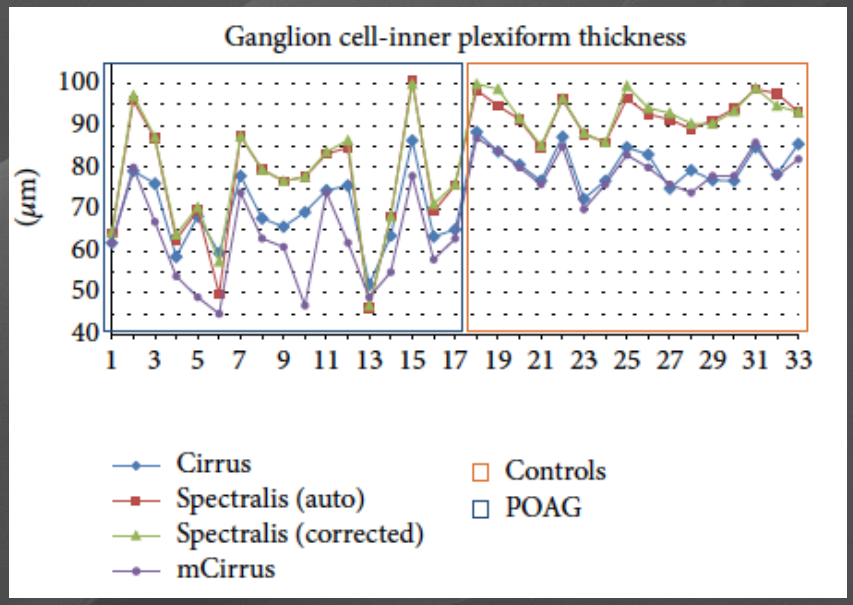

In conclusion, the significant difference between measurements from Cirrus and Spectralis OCTs does not allow free interchange of machines, for instance, in the follow-up of patients. In a clinical setting, clinicians must be aware that once you change the machine and software analysis, a new baseline for the patient is needed. Nevertheless both machines showed similar capability of diagnostic performance in early glaucoma and also in their correlation to functional changes such as standard automated perimetry.

Grazie per l'attenzione